

# Quantum Transport with Spin Dephasing: A Nonequilibrium Green's Function Approach

Ahmet Ali Yanik\*

*Department of Physics, and  
Network for Computational Nanotechnology,  
Purdue University, West Lafayette, IN, 47907, USA*

Gerhard Klimeck

*School of Electrical and Computer Engineering,  
Network for Computational Nanotechnology,  
Purdue University, West Lafayette, IN, 47907, USA and  
Jet Propulsion Lab, Caltech, Pasadena, CA, 91109, USA*

Supriyo Datta

*School of Electrical and Computer Engineering and  
Network for Computational Nanotechnology,  
Purdue University, West Lafayette, IN, 47907, USA*

(Dated: March 23, 2022)

A quantum transport model incorporating spin scattering processes is presented using the non-equilibrium Green's function (NEGF) formalism within the self-consistent Born approximation. This model offers a unified approach by capturing the spin-flip scattering and the quantum effects simultaneously. A numerical implementation of the model is illustrated for magnetic tunnel junction devices with embedded magnetic impurity layers. The results are compared with experimental data, revealing the underlying physics of the coherent and incoherent transport regimes. It is shown that small variations in magnetic impurity spin-states/concentrations could cause large deviations in junction magnetoresistances.

PACS numbers: 72.10.-d, 72.25.-b, 72.25.Rb, 71.70.Gm, 73.43.Qt

## I. INTRODUCTION

Quantum transport in spintronic devices is currently a topic of great interest. Most of the theoretical work reported so far has been based on the Landauer approach [1] assuming coherent transport, although a few authors have included incoherent processes through averaging over a large ensemble of disordered configurations [2, 3, 4]. However, it is not straightforward to include dissipative interactions in such approaches. The non-equilibrium Green's function (NEGF) formalism provides a natural framework for describing quantum transport in the presence of incoherent and dissipative processes. Here, a numerical implementation of the NEGF formalism with spin-flip scattering is presented. For magnetic tunnel junctions (MTJs) with embedded magnetic impurity layers, this model is able to capture and explain three distinctive experimental features reported in the literature [5, 6, 7, 8] regarding the dependence of the junction magnetoresistances (*JMRs*) on (1) barrier thickness, (2) barrier height and (3) the number of magnetic impurities. The model is quite general and can be used to analyse and design a variety of spintronic devices beyond the 1-D geometry explored in this article.

This article is organized as follows. In the view of pedagogical clarity, a heuristic presentation of the NEGF formalism with spin dephasing mechanisms is given Sec II followed by a numerical implementation of the model in Sec III. Initially (Sec III A) the definitions of device characteristics are presented for *impurity free* MTJs together with device parameters benchmarked against experimental measurements. How to incorporate the spin exchange scattering mechanisms into the electron transport calculations is shown (Sec III B), and the model is applied to MTJ devices with magnetic impurity layers (Sec III C). Theoretical estimates and experimental measurements are compared as well in this section (Sec III C), while a summary of the results is given in Sec IV.

## II. MODEL DESCRIPTION

*NEGF Method:* The problem is partitioned into channel and contact regions as illustrated in Fig. 1 [9]. Components of the partitioned device can be classified in four categories:

(i) *Channel* properties are defined by the Hamiltonian matrix  $[H]$  including the applied bias potential.

(ii) *Contacts* are included through self-energy matrices  $[\Sigma_L]/[\Sigma_R]$  whose anti-hermitian component:

$$\Gamma_{L,R}(E) = i \left( \Sigma_{L,R}(E) - \Sigma_{L,R}^\dagger(E) \right), \quad (1)$$

---

\*Electronic address: yanik@purdue.edu

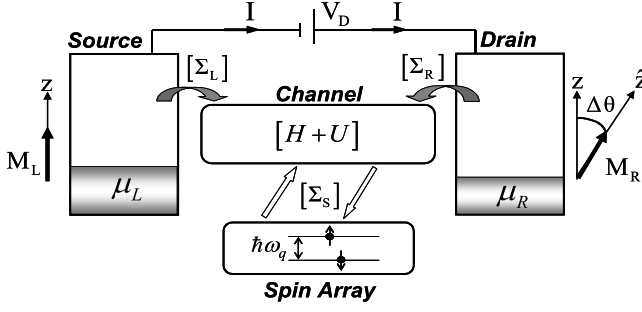


FIG. 1: A schematic illustration of device partitioning in NEGF formalism. Magnetization direction of the drain is defined relative to the source ( $\Delta\theta = \theta_R - \theta_L$ ).

describes the broadening due to the coupling to the contact. The corresponding inscattering/outscattering matrices are defined as:

$$\Sigma_{L,R}^{in}(E) = f_0(E - \mu_{L,R}) \Gamma_{L,R}(E), \quad (2a)$$

$$\Sigma_{L,R}^{out}(E) = [1 - f_0(E - \mu_{L,R})] \Gamma_{L,R}(E), \quad (2b)$$

where  $f_0(E - \mu_{L,R}) = 1 / (1 + \exp[(E - \mu_{L,R}) / k_B T])$  is the Fermi function for the related contact.

(iii) *Electron-electron interactions* are incorporated through the mean field electrostatic potential matrix  $[U]$ .

(iv) *Incoherent* scattering processes in the channel region are described by in/out-scattering matrices

$[\Sigma_S^{in}] / [\Sigma_S^{out}]$ . Broadening due to scattering is given by:

$$\Gamma_S(E) = [\Sigma_S^{in}(E) + \Sigma_S^{out}(E)], \quad (3)$$

from which the self-energy matrix is obtained through a Hilbert transform:

$$\Sigma_S(E) = \overbrace{\frac{1}{2\pi} \int \frac{\Gamma_S(E')}{E' - E} dE'}^{\text{Re}} - i \overbrace{\frac{\Gamma_S(E)}{2}}^{\text{Im}}. \quad (4)$$

Eqs. (1-2) are the boundary conditions that drive the coupled NEGF equations [Eqs. (3-8)], where Green's function is defined as:

$$G = [EI - H - U - \Sigma_L - \Sigma_R - \Sigma_S]^{-1}, \quad (5)$$

with the spectral function (analogous to density states):

$$A = i[G - G^\dagger] = G^n + G^p, \quad (6)$$

where  $[G^n] / [G^p]$  refer the *electron/hole correlation functions* (whose diagonal elements are the electron/hole density):

$$G^{n,p} = G [\Sigma_L^{in,out} + \Sigma_R^{in,out} + \Sigma_S^{in,out}] G^\dagger. \quad (7)$$

The in/out-scattering matrices  $[\Sigma_S^{in}] / [\Sigma_S^{out}]$  are related to the electron/hole correlation functions  $[G^n] / [G^p]$  through:

$$\begin{aligned} \Sigma_{S;\sigma_i\sigma_j}^{in,out}(r, r'; E) = & \int \sum_{\sigma_k, \sigma_l} \left[ D_{\sigma_i\sigma_j; \sigma_k\sigma_l}^{n,p}(r, r'; \hbar\omega) \right]_{sf} G_{\sigma_k\sigma_l}^{n,p}(r, r'; E \mp \hbar\omega) d(\hbar\omega) \\ & + \int \sum_{\sigma_k, \sigma_l} \left[ D_{\sigma_i\sigma_j; \sigma_k\sigma_l}^{n,p}(r, r'; \hbar\omega) \right]_{nsf} G_{\sigma_k\sigma_l}^{n,p}(r, r'; E) d(\hbar\omega). \end{aligned} \quad (8)$$

Here the spin indices  $(\sigma_k, \sigma_l)$  refer to the  $(2 \times 2)$  block diagonal elements of the on-site electron/hole correlation function which is related through the  $[D^n] / [D^p]$  tensors to the  $(\sigma_i, \sigma_j)$  spin components of the  $(2 \times 2)$  block diagonal of the in/out-scattering function. This term can be interpreted as in the following. The first part describes the process of spin-flip transitions (subscript sf) due to the spin-exchange scatterings in the channel region. The second part denotes the contributions of the spin-conserving exchange scatterings (subscript nsf for "no spin-flip") in the channel region. Both of the contributing parts are previously shown by Appelbaum[10] using a similar treatment. Here the  $[D^n] / [D^p]$  are fourth-order scattering tensors, describing the spatial correlation and the energy spectrum of the underlying mi-

croscopic *spin-dephasing* scattering mechanisms. These scattering tensors can be obtained from the spin scattering hamiltonian:

$$H_I(\vec{r}) = \sum_{R_j} J(\vec{r} - \vec{R}_j) \vec{\sigma} \cdot \vec{S}_j, \quad (9)$$

where  $\vec{r} / \vec{R}_j$  are the spatial coordinates and  $\vec{\sigma} / \vec{S}_j$  are the spin operators for the *channel electron / (j-th) magnetic impurity*. For point like exchange scattering processes, the scattering tensor for the first term in Eq. (8) corresponding to the spin-flip transitions is given by (see Appendix):

$$\begin{aligned}
& |\sigma_k \sigma_l\rangle \rightarrow \langle \sigma_i \sigma_j | \downarrow \\
& [D^{\text{n,p}}(r, r'; \hbar\omega)]_{\text{sf}} = \delta(r - r') \sum_{\omega_q} J^2 N_I(\omega_q) \begin{matrix} \langle \uparrow\uparrow | \\ \langle \downarrow\downarrow | \\ \langle \uparrow\downarrow | \\ \langle \downarrow\uparrow | \end{matrix} \begin{matrix} |\uparrow\uparrow\rangle & |\downarrow\downarrow\rangle & |\uparrow\downarrow\rangle & |\downarrow\uparrow\rangle \\ \left[ \begin{array}{cccc} 0 & F_{u,d}\delta(\omega \mp \omega_q) & 0 & 0 \\ F_{d,u}\delta(\omega \pm \omega_q) & 0 & 0 & 0 \\ 0 & 0 & 0 & 0 \\ 0 & 0 & 0 & 0 \end{array} \right] \end{matrix} . \quad (10)
\end{aligned}$$


---

Also, the no-spin flip component in Eq. (8) is given by:

$$\begin{aligned}
& |\sigma_k \sigma_l\rangle \rightarrow \langle \sigma_i \sigma_j | \downarrow \\
& [D^{\text{n,p}}(r, r'; \hbar\omega)]_{\text{nsf}} = \delta(r - r') \sum_{\omega_q} \frac{1}{4} J^2 N_I(\omega_q) [\delta(\omega - \omega_q)] \begin{matrix} \langle \uparrow\uparrow | \\ \langle \downarrow\downarrow | \\ \langle \uparrow\downarrow | \\ \langle \downarrow\uparrow | \end{matrix} \begin{matrix} |\uparrow\uparrow\rangle & |\downarrow\downarrow\rangle & |\uparrow\downarrow\rangle & |\downarrow\uparrow\rangle \\ \left[ \begin{array}{cccc} 1 & 0 & 0 & 0 \\ 0 & 1 & 0 & 0 \\ 0 & 0 & -1 & 0 \\ 0 & 0 & 0 & -1 \end{array} \right] \end{matrix} . \quad (11)
\end{aligned}$$


---

*Current* is calculated from the self-consistent solution of the above equations for any terminal "i":

$$I_i = \frac{q}{h} \int_{-\infty}^{\infty} \text{trace} ([\Sigma_i^{\text{in}}(E) A(E)] - [\Gamma_i(E) G^n(E)]) dE. \quad (12)$$

The general solution scheme without going into the details can be summarized as follows. The matrices listed under the categories (i) and (ii) are fixed at the outset of any calculations. While the  $[U]$ ,  $[\Sigma_S^{\text{in,out}}]$  and  $[\Sigma_S]$  matrices under the *charging and scattering* categories (iii) and (iv) depend on the correlation and spectral functions requiring an *iterative self-consistent solution* of the NEGF Equations [Eqs. (3-8)]. One important thing to note is that for the numerical implementation presented in Sec III we do not compute the charging potential  $[U]$  self-consistently with the charge. The change in tunnel barriers is neglected and assumed not to influence the electrostatic potential. This allows one to focus on the *dephasing* due to the spin-flip interactions.

### III. APPLICATION: MTJs WITH MAGNETIC IMPURITIES

In the presence of "rigid" scatterers such as impurities and defects, electron transport is considered coherent as the phase relationships between different paths are time independent. Accordingly, any static deviations from perfect crystallinity leading to the scattering of the electrons from one state to another can be incorporated into the transport problem through the device Hamiltonian  $H$ . However the situation is different when

the impurities have an internal degree of freedom, such as fluctuating internal spin states in the case of magnetic impurities. Electron scatterings from such impurities randomize the electron spin states which can not be simply incorporated through the device Hamiltonian. Instead scattering self energy matrices are needed for this type of phase-relaxing scattering processes. An implementation of this self-energy matrix treatment will be discussed in this part of the paper for electron-impurity exchange scattering processes in MTJs. But first, we'll discuss MTJ fundamentals and device characteristics in the absence of magnetic impurities (*the coherent regime*).

#### A. MTJs: Coherent Regime

MTJs devices considered here consist of a tunneling barrier ( $\text{AlO}_x$ ) sandwiched between two ferromagnets (Co) with different magnetic coercivities enabling independent manipulation of contact magnetization directions (Fig. 2). Single band tight-binding approxi-

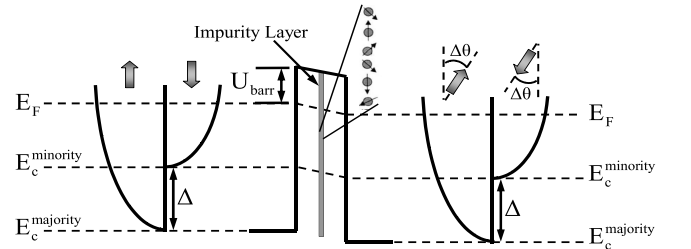


FIG. 2: Energy band diagram for the model MTJs considered here.

mation is adopted [11] with an effective electron mass ( $m^* = m_e$ ) in the tunneling region and the ferromagnetic contacts. Accordingly for constant effective mass throughout the device, transverse modes can be included using 2-D integrated Fermi functions  $f_{2D}(E_z - \mu_{L,R}) = (m^* k_B T / 2\pi \hbar^2) \ln [1 + \exp(\mu_{L,R} - E_z / k_B T)]$  in Eq. (2) instead of numerically summing parallel k-components. The Green's function of the device is simply defined as:

$$G(E_z) = (E_z I - H - \Sigma_L - \Sigma_R)^{-1}, \quad (13)$$

without any self-consistent solution requirements where  $H$  is Hamiltonian of the isolated system, and  $\Sigma_L/\Sigma_R$  are the self-energies due to the source/drain contacts. Here the matrices have twice the size of the channel region in the corresponding presentation due to the electron spin states. Accordingly, in real space representation for a discrete lattice whose points are located at  $x = ja$ ,  $j$  being an integer ( $j = 1 \cdots N$ ), the matrix  $(E_z I - H - \Sigma_L - \Sigma_R)$  can be expressed as:

$$E_z I - H - \Sigma_L - \Sigma_R = \begin{matrix} & \begin{matrix} |1\rangle & |2\rangle & & |N-1\rangle & |N\rangle \end{matrix} \\ \begin{matrix} \langle 1| \\ \langle 2| \\ \vdots \\ \langle N-1| \\ \langle N| \end{matrix} & \begin{bmatrix} E_z \bar{I} - \alpha_1 - \bar{\Sigma}_L & \beta & \cdots & \bar{0} & \bar{0} \\ E_z \bar{I} - \alpha_2 & \cdots & \bar{0} & \bar{0} & \bar{0} \\ \vdots & \ddots & \vdots & \vdots & \vdots \\ \bar{0} & \cdots & E_z \bar{I} - \alpha_{N-1} & \beta & \beta \\ \bar{0} & \cdots & \beta^+ & E_z \bar{I} - \alpha_N - \bar{\Sigma}_R \end{bmatrix} \end{matrix}, \quad (14)$$

where  $\alpha_n$  is a 2x2 on-site matrix:

$$\alpha_n = \begin{bmatrix} E_{c,n}^\uparrow + 2t + U_n & 0 \\ 0 & E_{c,n}^\downarrow + 2t + U_n \end{bmatrix}, \quad (15)$$

and  $\beta = -t\bar{I}$  is a 2x2 site-coupling matrix with  $t = \hbar^2/2ma^2$  and  $\bar{I} = \begin{pmatrix} 1 & 0 \\ 0 & 1 \end{pmatrix}$ . The left contact self-energy matrix is nonzero only for the first 2x2 block:

$$\Sigma_L(1,1;E_z) = \bar{\Sigma}_L = \begin{bmatrix} -te^{ik_L^\uparrow a} & 0 \\ 0 & -te^{ik_L^\downarrow a} \end{bmatrix}, \quad (16)$$

where  $E_z = E_c^{\uparrow,\downarrow} + U_L + 2t(1 - \cos k_L^{\uparrow,\downarrow} a)$ . For the right contact only the last block is non-zero:

$$\Sigma_R(N,N,E_z) = \bar{\Sigma}_R = \tilde{\mathfrak{R}} \begin{bmatrix} -te^{ik_R^\uparrow a} & 0 \\ 0 & -te^{ik_R^\downarrow a} \end{bmatrix} \tilde{\mathfrak{R}}^\dagger, \quad (17)$$

where  $E_z = E_c^{\uparrow,\downarrow} + U_R + 2t(1 - \cos k_R^{\uparrow,\downarrow} a)$  with  $\tilde{\mathfrak{R}}$  being the unitary rotation operator defined as:

$$\tilde{\mathfrak{R}}(\Delta\theta) = \begin{bmatrix} \cos(\Delta\theta/2) & \sin(\Delta\theta/2) \\ -\sin(\Delta\theta/2) & \cos(\Delta\theta/2) \end{bmatrix}, \quad (18)$$

for two contacts with magnetization directions differing by an angle  $\Delta\theta$ .

A *theoretical analysis* of MTJ devices in the absence of magnetic impurity layers is presented and compared with the experimental data [5, 7] for varying tunneling barrier heights and thicknesses. The parameters used here for the generic ferromagnetic contacts are the Fermi energy

$E_F = 2.2$  eV and the exchange field  $\Delta = 1.45$  eV [11]. The tunneling region potential barrier  $[U_{barr}]$  is parameterized within the band gaps quoted from the literature [12, 13], while the charging potential  $[U]$  is neglected due to the pure tunneling nature of the transport.

*Coherent* tunneling regime features are obtained by benchmarking the experimental measurements made in impurity free tunneling oxide MTJs at small bias voltages. Referring to  $I_F/I_{AF}$  as the current values for the parallel/antiparallel magnetizations ( $\Delta\theta = 0/\Delta\theta = \pi$ ) of the ferromagnetic contacts, the *JMR* is defined as:

$$JMR = (I_F - I_{AF})/I_F. \quad (19)$$

The dependence of the *JMRs* on the thickness and the height of the tunneling barriers is shown in Fig. 3(a) with an energy resolved analysis [Fig. 3(b)] for different barrier thicknesses (0.7 – 1.4 – 2.1 nm). *JMR* values are shown to be improving with increasing barrier heights for all barrier thicknesses, a theoretically predicted [7, 8, 14] and experimentally observed [15, 16, 17, 18, 19, 20, 21, 22, 23, 24] feature in MTJs. The barrier heights obtained here may differ from those reported in literature [15, 16, 17, 18, 19, 20, 21, 22, 23, 24] based on empirical models [25].

Experiments and theoretical calculations observe deterioration of *JMRs* with increasing barrier thicknesses [Fig. 3(a)]. Whereas an energy resolved theoretical analysis shows that energy by energy junction magnetoresistances defined as:

$$JMR(E_z) = (I_F(E_z) - I_{AF}(E_z))/I_F(E_z), \quad (20)$$

remain unchanged [Fig. 3(b)]. This initially counter intuitive observation can be understood by considering the

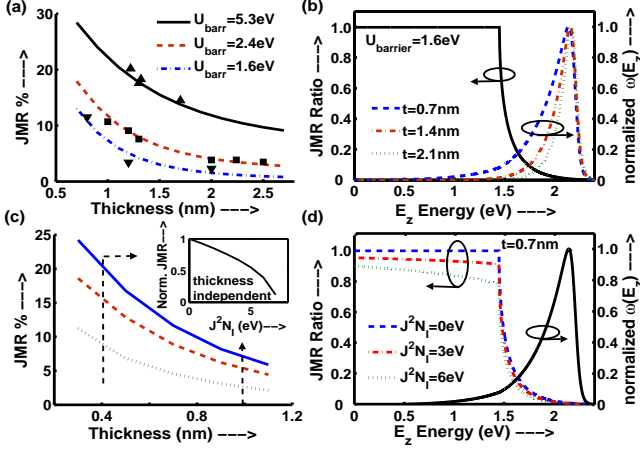


FIG. 3: For impurity free MTJs, (a) thickness dependence of  $JMR$ s for different barrier heights are shown in comparison with experimental measurements [15, 16, 17, 18, 19, 20, 21, 22, 23, 24] while an (b) energy resolved analysis of  $JMR(E_z)$  (left-axis) and  $normalized\ w(E_z)$  (right-axis) distributions is also presented for a device with a tunneling barrier height of  $1.6\text{ eV}$ . For MTJs with impurity layers, (c) variation of  $JMR$ s for varying barrier thicknesses and interactions strengths are shown together with (d) an energy resolved analysis. Normalized  $JMR$ s are proven to be thickness independent as displayed in the inset.

redistribution of tunneling electron densities over energies with changing tunneling barrier thicknesses. Defining  $w(E_z)$  as a measure of the contributing weight of the  $JMR(E_z)$ , one can show that experimentally measured  $JMR$  is a weighted integral of  $JMR(E_z)$ s over  $E_z$  energies:

$$JMR = \int \omega(E_z) JMR(E_z) dE_z, \quad (21)$$

where  $\omega(E_z) = I_F(E_z)/I_F$  is the energy resolved *spin-continuum current component* (weighting function). In Eq. (21), independently from the barrier thicknesses  $JMR(E_z)$  ratios are *constant* (solid line in Fig. 3(b)), while the *normalized  $w(E_z)$*  distributions shifts towards higher energies with increasing barrier thicknesses (dashed lines in Fig. 3(b)). Hence  $JMR$ s, an integral of the multiplication of the  $w(E_z)$  distributions with the energy resolved  $JMR(E_z)$ s, decreases with increasing barrier thicknesses (Eq. (19)).

## B. Adding Spin Exchange Scattering

Spin exchange scattering processes are responsible from the incoherent nature of the tunneling transport for the model devices considered here. Through this elastic scattering process, the state of nothing else seem to change if the electron and the impurity spins are considered as a composite system. Nevertheless, it is an incoherent process since the state of the impurity has changed. What makes this process incoherent are the external forces forcing the impurity spins into local equilibrium. The incoherent nature of the scattering lies in the "information erasure" of the surrounding through the forces forcing the impurity spins into an unpolarized (%50 up, %50 down) spin distribution. These external forces in a closely packed impurity layer can be magnetic dipole-dipole interactions among the magnetic impurities or spin relaxation processes coupled with phononic excitations. Nevertheless the physical origin of the equilibrium restoring processes is not of our interest (at least from tunneling electron's point of view) assuming equilibrium restoring processes are fast enough to maintain the impurity spins in a thermal equilibrium state. Accordingly, NEGF formalism incorporates spin dephasing effects of the environment into the electron transport problem through a boundary condition (the spin-scattering self-energy). As discussed in Sec II, coupling between the number of available electrons/holes ( $[G^n]/[G^p]$ ) at a state and the in/out-flow ( $[\Sigma_S^{in}]/[\Sigma_S^{out}]$ ) to/from that state is related through the fourth order scattering tensor  $[D^n]/[D^p]$  in Eq. (8).

For the model systems considered here magnetic impurity spin states are degenerate ( $\hbar\omega_q = 0$ ) allowing only elastic spin-flip transitions. Spin-conserving scattering processes are also neglected due to their minor effect on the  $JMR$ s. Accordingly, the spin scattering tensor relationship given in Eqs. (8,10 and 11) will simplify to:

$$\Sigma_S^{in,out}(r, r; E) = \left[ D_{\sigma_i \sigma_j; \sigma_k \sigma_l}^{n,p} \right]_{sf} G_{\sigma_k \sigma_l}^{n,p}(r, r; E). \quad (22)$$

$[D^n]/[D^p]$  scattering tensors relate the electron/hole  $[G^n]/[G^p]$  correlation matrices with the (2x2) block diagonal elements of  $[\Sigma_S^{in}]/[\Sigma_S^{out}]$  in/out-scattering matrices of form:

$$\Sigma_S^{in,out} = \begin{pmatrix} (\bar{\Sigma}_S^{in,out})_{1,1} & \bar{0} & \cdots & \bar{0} \\ \bar{0} & (\bar{\Sigma}_S^{in,out})_{2,2} & \cdots & \bar{0} \\ \vdots & \vdots & \ddots & \vdots \\ \bar{0} & \bar{0} & \cdots & (\bar{\Sigma}_S^{in,out})_{N,N} \end{pmatrix}, \quad (23)$$

through the tensor relationship (*shown below in matrix format*) for the corresponding lattice site "j" with magnetic impurities:

$$\begin{bmatrix} (\Sigma_{S;\uparrow\uparrow}^{in,out})_{jj} \\ (\Sigma_{S;\downarrow\downarrow}^{in,out})_{jj} \\ (\Sigma_{S;\uparrow\downarrow}^{in,out})_{jj} \\ (\Sigma_{S;\downarrow\uparrow}^{in,out})_{jj} \end{bmatrix} = J^2 N_I \overbrace{\begin{bmatrix} 0 & F_{u,d} & 0 & 0 \\ F_{d,u} & 0 & 0 & 0 \\ 0 & 0 & 0 & 0 \\ 0 & 0 & 0 & 0 \end{bmatrix}}^{[D^{n,p}]_{sf}} \begin{bmatrix} (G_{\uparrow\uparrow}^{n,p})_{jj} \\ (G_{\downarrow\downarrow}^{n,p})_{jj} \\ (G_{\uparrow\downarrow}^{n,p})_{jj} \\ (G_{\downarrow\uparrow}^{n,p})_{jj} \end{bmatrix}, \quad (24)$$

where  $N_I$  is the number of magnetic impurities and  $F_u/F_d$  represents fractions of spin-up/spin-down impurities for an uncorrelated ensemble ( $F_u + F_d = 1$ ).

This tensor relationship can be understood heuristically from elementary arguments. The in/out-scattering into *spin-up* component is proportional to the density of the *spin-down electrons/holes* times the number of *spin-up impurities*,  $N_I F_u$ :

$$(\Sigma_{S;\uparrow\uparrow}^{in,out})_{jj} = J^2 N_I F_u (G_{\downarrow\downarrow}^{n,p})_{jj}. \quad (25)$$

Similarly, the in/out-scattering into *spin-down* component is proportional to the density of the *spin-up electrons/holes* times the number of *spin-down impurities*,  $N_I F_d$ :

$$(\Sigma_{S;\downarrow\downarrow}^{in,out})_{jj} = J^2 N_I F_d (G_{\uparrow\uparrow}^{n,p})_{jj}. \quad (26)$$

### C. Incoherent Regime: Results

The *incoherent* tunneling regime device characteristics in the presence of magnetic impurities is studied for a fixed barrier height  $U_{barr} = 1.6$  eV [Fig. 3 (c)] with changing barrier thicknesses and electron-impurity spin exchange interactions ( $J^2 N_I = 0 - 6$  eV). *Nonlinear* decreasing *JMRs* with increasing spin-exchange interactions are observed at all barrier thicknesses due to the mixing of independent spin-channels [5, 6] while the *normalized JMRs* are proven to be thickness independent (*inset*). This observation is attributed to the elastic nature of the spin exchange interactions yielding a total drop in  $JMR(E_z)$  values at all  $E_z$  energies in Eq. (19)

while preserving the *normalized*  $\omega(E_z)$  carrier distributions [Fig. 3(d)].

Further analysis shows that "*normalized*" *JMRs* deteriorates with increasing spin-dephasing strenghts ( $J^2 N_I$ ) independently from the tunneling barrier heights [Fig. 4(a)]. This general trend can be shown by mapping the "*normalized*" *JMRs* into a *single universal curve* using a tunneling barrier height dependent scaling constant  $c(U_{barr})$  (inset in Fig. 4(a)).

This allows us to choose a particular value of barrier height [ $U_{barr} = 1.6$  eV] and adjust a *single parameter*  $J$  to fit our NEGF calculations [Fig. 4(b-d)] with experimental measurements obtained from  $\delta$ -doped MTJs [5]. Submonolayer impurity thicknesses given in the measurements are converted into number of impurities using material concentrations of Pd/Ni/Co impurities and device cross sections ( $6 \times 10^{-4}$  cm<sup>2</sup>) [5].

*Close fitting* to the experimental data are observed at 77K [Fig. 4(b-d)] using physically reasonable exchange coupling constants of  $J = 2.63 \mu\text{eV}/2.68 \mu\text{eV}/1.41 \mu\text{eV}$  for devices with Pd/Ni/Co impurities [26]. However, experimentally observed temperature dependence of *normalized*

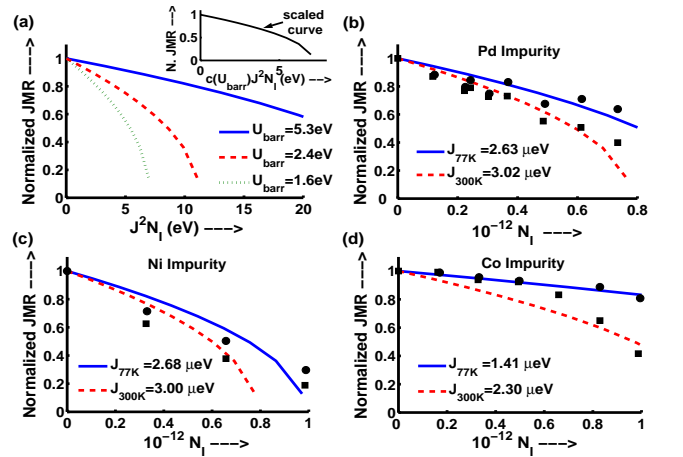


FIG. 4: (a) *Normalized JMRs* deteriorates with increasing spin-dephasing strenghts independently from the tunneling barrier heights. This general trend can be scaled to a *single universal curve* (inset). Experimental data taken at 77K and 300K is compared with theoretical analysis in the presence of (b) Pd, (c) Ni and (d) Co magnetic impurities with increasing impurity concentrations.

$JMR$  ratios can not be accounted for by our model calculations. Broadenings of the electrode Fermi distributions due to changing temperatures from 77K to 300K seem to yield variations in *normalized*  $JMR$  ratios within a linewidth. As a result, different  $J$  exchange couplings are used in order to match the experimental data taken at 300K.

For *Pd and Ni doped* MTJs, relatively small variations in  $J$  exchange couplings are needed ( $J_{300}/J_{77} = 1.16$  for Pd and  $J_{300}/J_{77} = 1.19$  for Ni) in order to match the experimental data at 300K. These small temperature dependences could be due to the presence of some secondary mechanisms not included in our calculations. One such mechanism reported in literature includes the presence of impurity-assisted conductance contribution through the defects (*possibly created by the inclusion of magnetic impurities within the barrier*) which is known to be strongly temperature dependent [27]. In fact, the contribution of the impurity-assisted conductance is proportional with the impurity concentrations in accordance with the experimental measurements.

Another interesting feature observed in calculations [Fig. 4(b-c)] is the comparable  $J$  exchange couplings for the Pd and Ni impurities at temperatures 77K and 300K. Accordingly, a possible estimate of the impurity spin states may be made by considering the most commonly encountered oxidation states of the Pd and Ni impurities. Closed-shell elemental Pd is only known to be in a magnetic oxidized state of  $S=1$  in octahedral oxygen coordination according to the Hund's rules [28]. Similarly, we may attribute the comparable  $J$  couplings for Ni impurities due to the  $S=1$  spin state of the  $Ni^{+2}$  which is known to be a frequently observed ionized state in oxygen environment [29].

On the contrary, for *Co doped* MTJs, there's a clear distinction for *normalized*  $JMR$  ratios at different temperatures [Fig. 4(d)] which can not be justified by the presence of secondary mechanisms. Fitting these large deviations require large variations in  $J$  exchange coupling parameters [ $J_{300}/J_{77} = 1.73$ ]. We propose this to be a result of thermally driven *low-spin/high-spin phase* transition [30, 31]. This is a credible argument since the oxidation state of the cobalt atoms can be in  $Co^{+2}$  ( $S = 3/2$ , high-spin) or  $Co^{+3}$  ( $S = 0$ , low-spin) state or partially in both of the states depending on the oxidation environment. Such thermally driven low-spin/high-spin phase transitions for metal-oxides have been predicted by theoretical calculations and observed in experimental studies [30, 31]. These phase transitions have not been discussed in MTJs community in connection with possible scattering factors determining the temperature dependence of  $JMRs$ . Although from the available experimental data it's not possible to make a decisive conclusion in this direction, given the *nonlinear* dependence of  $JMRs$  on magnetic impurity states in our calculations, we believe that it's important to point out this possibility here.

## IV. SUMMARY

*Summary:* A NEGF based quantum transport model incorporating spin-flip scattering processes within the self-consistent Born approximation is presented. Spin-flip scattering and quantum effects are simultaneously captured. Spin scattering operators are derived for the specific case of electron-impurity spin-exchange interactions and the formalism is applied to spin dependent electron transport in MTJs with magnetic impurity layers. The theory is benchmarked against experimental data involving both coherent and incoherent transport regimes.  $JMRs$  are shown to decrease both with barrier thickness and with spin-flip scattering but our unified treatment clearly brings out the difference in the underlying physics [Fig. 3]. Our numerical results show that both barrier height and the exchange interaction constant  $J$  can be subsumed into a single parameter that can explain a variety of experiments [Fig. 4(a)]. Nonlinear dependence of  $JMR$  ratios on the impurity concentrations are shown [Fig. 4(b-d)] in difference with earlier linear estimates from empirical models [5]. Accordingly, small differences in spin-states/concentrations of magnetic impurities are shown to cause large deviations in  $JMRs$ . Interesting similarities and differences among devices having Pd, Ni and Co impurities are pointed out, which could be signatures of the spin states of oxidized Pd and Ni impurities and low-spin/high-spin phase transitions for oxidized cobalt impurities.

## Acknowledgments

This work was supported by the MARCO focus center for Materials, Structure and Devices and the NSF Network for Computational Nanotechnology. Part of this work was carried out at the Jet Propulsion Laboratory under a contract with the National Aeronautics and Space Administration NASA funded by ARDA.

## APPENDIX: SPIN DEPHASING SELF ENERGY

In the following, the scattering tensors stated in Eqs. (10-11) of the main paper are obtained starting from standard expressions obtained in the self-consistent Born approximation from the NEGF formalism. Here we start from the formulation in Ref. 9 (see Sections 10.4 and A.4) which represents a generalization of the earlier treatments [32, 33, 34, 35]. For spatially localized scatterers we have:

$$H_{I;\sigma_l\sigma_j}(t) = \langle \sigma_l | H_I(t) | \sigma_j \rangle \quad (\text{A.2b})$$

$$\begin{aligned} D_{\sigma_i\sigma_j;\sigma_k\sigma_l}^n(t, t') &= \left\langle \sum_{s_\beta, s_\alpha} \tau_{\sigma_i s_\alpha; \sigma_k s_\beta}(t) \tau_{\sigma_j s_\alpha; \sigma_l s_\beta}^*(t') \right\rangle \\ &= \left\langle \sum_{s_\alpha, s_\beta} \langle s_\alpha | H_{I;\sigma_i\sigma_k}(t) | s_\beta \rangle \langle s_\beta | H_{I;\sigma_l\sigma_j}^\dagger(t') | s_\alpha \rangle \right\rangle \quad (\text{A.1a}) \end{aligned}$$

$$\begin{aligned} D_{\sigma_i\sigma_j;\sigma_k\sigma_l}^p(t, t') &= \left\langle \sum_{s_\beta, s_\alpha} \tau_{\sigma_l s_\beta; \sigma_j s_\alpha}(t) \tau_{\sigma_k s_\beta; \sigma_i s_\alpha}^*(t') \right\rangle \\ &= \left\langle \sum_{s_\alpha, s_\beta} \langle s_\beta | H_{I;\sigma_l\sigma_j}(t) | s_\alpha \rangle \langle s_\alpha | H_{I;\sigma_i\sigma_k}^\dagger(t') | s_\beta \rangle \right\rangle \quad (\text{A.1b}) \end{aligned}$$

where  $|s_\alpha\rangle$  and  $|s_\beta\rangle$  are *impurity spin subspace* states and  $H_I$  is the interaction Hamiltonian [Eq. (9)] defined within the channel *electron spin subspace* as:

$$H_{I;\sigma_i\sigma_k}(t) = \langle \sigma_i | H_I(t) | \sigma_k \rangle \quad (\text{A.2a})$$

$$H_{I;\sigma_i\sigma_k}^\dagger(t') = \langle \sigma_i | H_I^\dagger(t') | \sigma_k \rangle \quad (\text{A.2c})$$

$$H_{I;\sigma_l\sigma_j}^\dagger(t') = \langle \sigma_l | H_I^\dagger(t') | \sigma_j \rangle \quad (\text{A.2d})$$

For an uncorrelated impurity spin ensemble with:

$$\rho = \sum_{s_\alpha} w_{s_\alpha} |s_\alpha\rangle \langle s_\alpha| = \sum_{s_\beta} w_{s_\beta} |s_\beta\rangle \langle s_\beta| \quad (\text{A.3})$$

averaging in Eqs. (A.1a-A.1b) can be done through a weighted summation of spin scattering rates of magnetic impurities:

$$\begin{aligned} D_{\sigma_i\sigma_j;\sigma_k\sigma_l}^n(t, t') &= \sum_{s_\alpha, s_\beta} w_{s_\beta} \langle s_\alpha | H_{I;\sigma_i\sigma_k}(t) | s_\beta \rangle \langle s_\beta | H_{I;\sigma_l\sigma_j}^\dagger(t') | s_\alpha \rangle \\ &= \sum_{s_\alpha} \langle s_\alpha | H_{I;\sigma_i\sigma_k}(t) [\rho] H_{I;\sigma_l\sigma_j}^\dagger(t') | s_\alpha \rangle = \text{tr} \left( \rho H_{I;\sigma_l\sigma_j}^\dagger(t') H_{I;\sigma_i\sigma_k}(t) \right) \quad (\text{A.4a}) \end{aligned}$$

$$\begin{aligned} D_{\sigma_i\sigma_j;\sigma_k\sigma_l}^p(t, t') &= \sum_{s_\alpha, s_\beta} w_{s_\alpha} \langle s_\beta | H_{I;\sigma_l\sigma_j}(t) | s_\alpha \rangle \langle s_\alpha | H_{I;\sigma_i\sigma_k}^\dagger(t') | s_\beta \rangle \\ &= \sum_{s_\beta} \langle s_\beta | H_{I;\sigma_l\sigma_j}(t) [\rho] H_{I;\sigma_i\sigma_k}^\dagger(t') | s_\beta \rangle = \text{tr} \left( \rho H_{I;\sigma_i\sigma_k}^\dagger(t') H_{I;\sigma_l\sigma_j}(t) \right) \quad (\text{A.4b}) \end{aligned}$$

The trace  $\text{tr}(\rho A)$  for any operator  $A$  is independent of representation. Accordingly,  $[D^n]/[D^p]$  scattering tensors can be evaluated using any convenient basis for magnetic impurity spin states.

Through Jordan-Wigner transformation, single spins can be thought as an empty or singly occupied fermion state:

$$|\uparrow\rangle \equiv a^\dagger |0\rangle, \quad (\text{A.5a})$$

$$|\downarrow\rangle \equiv |0\rangle, \quad (\text{A.5b})$$

with *creation/annihilation* operators for the channel electrons:

For degenerate electron spin states ( $\hbar\omega_e = 0$ ), there's no time dependence as such  $a^\dagger(t) \rightarrow a^\dagger$ ,  $a(t) \rightarrow a$ .

Pauli spin matrices are related to creation/annihilation operators through  $\sigma_x = (a^\dagger + a)/2$ ,  $\sigma_y = (a^\dagger - a)/2i$  and  $\sigma_z = a^\dagger a - 1/2$ . Accordingly, interaction Hamiltonian  $H_I(\vec{r}, t) = J\delta(\vec{r} - \vec{R}) \vec{\sigma} \cdot \vec{S}(t)$  can be expressed as:

$$a^+(t) = \sigma^+(t) = \begin{bmatrix} 0 & e^{i\omega_e t} \\ 0 & 0 \end{bmatrix}, \quad (\text{A.6a})$$

$$a(t) = \sigma^-(t) = \begin{bmatrix} 0 & 0 \\ e^{-i\omega_e t} & 0 \end{bmatrix}. \quad (\text{A.6b})$$



$$H_I(\vec{r}, t) = J\delta(\vec{r} - \vec{R}) \left[ \frac{1}{2}aS_+(t) + \frac{1}{2}a^\dagger S_-(t) + \left(a^\dagger a - \frac{1}{2}\right) S_Z(t) \right], \quad (\text{A.7})$$

where S is the spin operator for the localized magnetic impurity.

Substituting the interaction Hamiltonian from Eq. (A.7) into Eqs. (A.4a-A.4b) will yield:

$$H_{I;\sigma_l\sigma_j}^\dagger(t') H_{I;\sigma_i\sigma_k}(t) = \begin{matrix} |\sigma_k\sigma_l\rangle \rightarrow \\ \langle\sigma_i\sigma_j| \downarrow \end{matrix} \begin{matrix} |\uparrow\uparrow\rangle & |\downarrow\downarrow\rangle & |\uparrow\downarrow\rangle & |\downarrow\uparrow\rangle \end{matrix} \begin{matrix} \langle\uparrow\uparrow| \\ \langle\downarrow\downarrow| \\ \langle\uparrow\downarrow| \\ \langle\downarrow\uparrow| \end{matrix} \begin{bmatrix} S_Z(t') S_Z(t) & S_+(t') S_-(t) & S_+(t') S_Z(t) & S_Z(t') S_-(t) \\ S_-(t') S_+(t) & S_Z(t') S_Z(t) & -S_Z(t') S_+(t) & -S_-(t') S_Z(t) \\ S_-(t') S_Z(t) & -S_Z(t') S_-(t) & -S_Z(t') S_Z(t) & S_-(t') S_-(t) \\ S_Z(t') S_+(t) & -S_+(t') S_Z(t) & S_+(t') S_+(t) & -S_Z(t') S_Z(t) \end{bmatrix}, \quad (\text{A.8a})$$

$$H_{I;\sigma_l\sigma_k}^\dagger(t') H_{I;\sigma_l\sigma_j}(t) = \begin{matrix} |\sigma_k\sigma_l\rangle \rightarrow \\ \langle\sigma_i\sigma_j| \downarrow \end{matrix} \begin{matrix} |\uparrow\uparrow\rangle & |\downarrow\downarrow\rangle & |\uparrow\downarrow\rangle & |\downarrow\uparrow\rangle \end{matrix} \begin{matrix} \langle\uparrow\uparrow| \\ \langle\downarrow\downarrow| \\ \langle\uparrow\downarrow| \\ \langle\downarrow\uparrow| \end{matrix} \begin{bmatrix} S_Z(t') S_Z(t) & S_-(t') S_+(t) & S_Z(t') S_+(t) & S_-(t') S_Z(t) \\ S_+(t') S_-(t) & S_Z(t') S_Z(t) & -S_+(t') S_Z(t) & -S_Z(t') S_-(t) \\ S_Z(t') S_-(t) & -S_-(t') S_Z(t) & -S_Z(t') S_Z(t) & S_-(t') S_-(t) \\ S_+(t') S_Z(t) & -S_Z(t') S_+(t) & S_+(t') S_+(t) & -S_Z(t') S_Z(t) \end{bmatrix}, \quad (\text{A.8b})$$

The localized magnetic impurity spin-operators can be written in its diagonalized *impurity spin-subspace* as:

$$S_+ = d^\dagger = \begin{bmatrix} 0 & e^{i\omega_q t} \\ 0 & 0 \end{bmatrix} \quad (\text{A.9a})$$

$$S_- = d = \begin{bmatrix} 0 & 0 \\ e^{-i\omega_q t} & 0 \end{bmatrix} \quad (\text{A.9b})$$

$$S_Z = d^\dagger d - \frac{1}{2} = \frac{1}{2} \begin{bmatrix} 1 & 0 \\ 0 & -1 \end{bmatrix} \quad (\text{A.9c})$$

with  $\omega_q = \Delta E_I / \hbar$  where  $\Delta E_I$  is the energy difference between spin-up and spin-down states for the localized magnetic impurities.

For a given impurity density matrix of the form (Fu+Fd=1):

$$\rho = N_I(\omega_q) \begin{bmatrix} F_u & 0 \\ 0 & F_d \end{bmatrix}, \quad (\text{A.10})$$

with  $N_I$  being total number of impurities, the desired quantities  $[D^n]/[D^p]$  can be obtained by evaluating the expectation values of the operators in Eqs. (A.8a) and (A.8b). Here the only non-zero elements are:

$$\text{tr}(\rho S_Z(t') S_Z(t)) = \frac{1}{2}, \quad (\text{A.11a})$$

$$\text{tr}(\rho S_+(t') S_-(t)) = F_u e^{-i\omega_q(t-t')}, \quad (\text{A.11b})$$

$$\text{tr}(\rho S_-(t') S_+(t)) = F_d e^{i\omega_q(t-t')}. \quad (\text{A.11c})$$

Finally, for a given impurity density matrix [Eq (A.10)],  $[D^n]/[D^p]$  tensors are obtained as:

$$D^n(t, t') = \sum_{\omega_q} J^2 N_I(\omega_q) \begin{matrix} |\sigma_k\sigma_l\rangle \rightarrow \\ \langle\sigma_i\sigma_j| \downarrow \end{matrix} \begin{matrix} |\uparrow\uparrow\rangle & |\downarrow\downarrow\rangle & |\uparrow\downarrow\rangle & |\downarrow\uparrow\rangle \end{matrix} \begin{matrix} \langle\uparrow\uparrow| \\ \langle\downarrow\downarrow| \\ \langle\uparrow\downarrow| \\ \langle\downarrow\uparrow| \end{matrix} \begin{bmatrix} 1/4 & F_u e^{-i\omega_q(t-t')} & 0 & 0 \\ F_d e^{i\omega_q(t-t')} & 1/4 & 0 & 0 \\ 0 & 0 & -1/4 & 0 \\ 0 & 0 & 0 & -1/4 \end{bmatrix}, \quad (\text{A.12a})$$

$$\begin{aligned}
& |\sigma_k \sigma_l\rangle \rightarrow \\
& \langle \sigma_i \sigma_j | \downarrow \\
& D^p(t, t') = \sum_{\omega_q} J^2 N_I(\omega_q) \begin{matrix} \langle \uparrow \uparrow | \\ \langle \downarrow \downarrow | \\ \langle \uparrow \downarrow | \\ \langle \downarrow \uparrow | \end{matrix} \left[ \begin{matrix} & |\uparrow \uparrow\rangle & |\downarrow \downarrow\rangle & |\uparrow \downarrow\rangle & |\downarrow \uparrow\rangle \\ F_u e^{-i\omega_q(t-t')} & 1/4 & F_d e^{i\omega_q(t-t')} & 0 & 0 \\ 0 & 0 & 0 & -1/4 & 0 \\ 0 & 0 & 0 & 0 & -1/4 \end{matrix} \right], \quad (\text{A.12b})
\end{aligned}$$

It's convenient to work with the Fourier transformed functions as such  $(t - t') \rightarrow \hbar\omega$ :

$$e^{-i\omega_q(t-t')} e^{-\eta|t-t'|/\hbar} \rightarrow \delta(\hbar\omega - \hbar\omega_q) \quad (\text{A.13})$$

where  $\eta$  being a positive infinitesimal. With Fourier transforming Eqs. (A.12a-A.12b) will simplify to

Eqs. (10-11) [35]. For the calculations reported in this article, diagonal elements not leading to spin-dephasing are omitted due to their negligible effect on  $JMR$  ratios. In this case  $[D^n]/[D^p]$  scattering tensors simplifies to a form (Eq. (24)) which can be understood from simple common-sense arguments (Eqs. (25) and (26)).

- 
- [1] R. Landauer, Physica Scripta **T42**, 110 (1992).
  - [2] Y. Li and C. R. Chang, Phys. Lett. A **287**, 415 (2001).
  - [3] Y. Li, C. R. Chang, and Y. D. Yao, J. Appl. Phys. **91**, 8807 (2002).
  - [4] L. Sheng, D. Y. Xing, and D. N. Sheng, Phys. Rev. B **69**, 132414 (2004).
  - [5] R. Jansen and J. S. Moodera, J. of Appl. Phys. **83**, 6682 (1998).
  - [6] R. Jansen and J. S. Moodera, Phys. Rev. B **61**, 9047 (1998).
  - [7] A. H. Davis, Ph.D. thesis, Tulane University (1994).
  - [8] A. H. Davis and J. M. Maclaren, J. Phys.: Condens. Matter **14**, 4365 (2002).
  - [9] S. Datta, *Quantum Transport: Atom to Transistor* (Cambridge University Press, Cambridge, 2005).
  - [10] J. Appelbaum, Phys. Rev. **154**, 633 (1967).
  - [11] M. B. Stearns, J. Magn. Magn. Mater. **5**, 167 (1977).
  - [12] J. S. Moodera and L. R. Kinder, Phys. Rev. Lett. **74**, 3273 (1995).
  - [13] V. E. Henrich and P. A. Cox, *The Surface Science of Metal Oxides* (Cambridge University Press, Cambridge, 1994).
  - [14] J. Mathon, Phys. Rev. B **56**, 11810 (1997).
  - [15] K. Matsuda, A. Kamijo, T. Mitsuzuka, and H. Tsuge, J. of Appl. Phys. **85**, 5261 (1999).
  - [16] H. Chen, Q. Y. Xu, G. Ni, J. Lu, H. Sang, S. Y. Zhang, and Y. W. Du, J. of Appl. Phys. **85**, 5798 (1999).
  - [17] J. Zhang and R. M. White, J. of Appl. Phys. **83**, 6512 (1998).
  - [18] T. Mitsuzuka, K. Matsuda, A. Kamijo, and H. Tsuge, J. of Appl. Phys. **85**, 5807 (1998).
  - [19] W. Oepts, H. J. Verhagen, R. Coehoorn, and W. J. M. de Jonge, J. of Appl. Phys. **86**, 3863 (1999).
  - [20] R. S. Beech, J. Anderson, J. Daughton, B. A. Everitt, and D. Wang, IEEE Trans. Mag. **32**, 4713 (1996).
  - [21] H. Yamanaka, K. Saito, K. Takanashi, and H. Fujimori, IEEE Trans. Mag. **35**, 2883 (1999).
  - [22] J. S. Moodera, J. Nowak, and R. J. M. van de Veerdonk, Phys. Rev. Lett. **80**, 2941 (1998).
  - [23] J. J. Sun and P. P. Freitas, J. of Appl. Phys. **85**, 5264 (1999).
  - [24] C. H. Shang, J. Nowak, R. Jansen, and J. S. Moodera, Phys. Rev. B **58**, 2917 (1998).
  - [25] J. G. Simmons, J. Appl. Phys. **34**, 1793 (1963).
  - [26] B. E. Kane, Nature **393**, 133 (1998).
  - [27] R. C. S. et al., J. of Appl. Phys. **85**, 5258 (1999).
  - [28] P. A. Cox, *Transition Metal Oxides. An Introduction to their Electronic Structure and Properties* (Clarendon, Oxford, 1992).
  - [29] S. Geschwind and J. P. Remeika, J. of Appl. Phys. **33**, 370 (1962).
  - [30] T. Kambara, J. Chem. Phys. **70**, 4199 (1979).
  - [31] S. W. Biernacki and B. Clerjaud, Phys. Rev. B **72**, 024406 (2005).
  - [32] R. Lake, G. Klimeck, R. C. Bowen, and D. Jovanovic, J. of Appl. Phys. **81** (1997).
  - [33] S. Datta, J. Phys.: Condens. Matter **2** (1990).
  - [34] G. D. Mahan, Phys. Rep. **145**, 251 (1987).
  - [35] S. Datta, Proc. of Inter. School of Phys. Societa Italiana di Fisica p. 244 (2004).